



**HAL**  
open science

## The Aquitaine Shelf Edge (Bay of Biscay): A Primary Outlet for Microbial Methane Release

Stéphanie Dupré, B. Loubrieu, Catherine Pierre, C. Scalabrin, C. Guérin, A. Ehrhold, A. Ogor, E. Gautier, L. Ruffine, R. Biville, et al.

► **To cite this version:**

Stéphanie Dupré, B. Loubrieu, Catherine Pierre, C. Scalabrin, C. Guérin, et al.. The Aquitaine Shelf Edge (Bay of Biscay): A Primary Outlet for Microbial Methane Release. *Geophysical Research Letters*, 2020, 47 (7), 10.1029/2019gl084561 . hal-03147369

**HAL Id: hal-03147369**

**<https://hal.science/hal-03147369v1>**

Submitted on 2 Mar 2021

**HAL** is a multi-disciplinary open access archive for the deposit and dissemination of scientific research documents, whether they are published or not. The documents may come from teaching and research institutions in France or abroad, or from public or private research centers.

L'archive ouverte pluridisciplinaire **HAL**, est destinée au dépôt et à la diffusion de documents scientifiques de niveau recherche, publiés ou non, émanant des établissements d'enseignement et de recherche français ou étrangers, des laboratoires publics ou privés.

# Geophysical Research Letters

## RESEARCH LETTER

10.1029/2019GL084561

### Key Points:

- Up to 2,612 gas bubbling sites at the Aquitaine Shelf edge release 144 Mg/yr of microbial methane into the water column
- Methane-derived authigenic (sub) outcropping carbonates cover 375 km<sup>2</sup>
- Methane-rich fluids have been circulating for at least a few thousand years

### Supporting Information:

- Supporting Information S1

### Correspondence to:

S. Dupré,  
stephanie.dupre@ifremer.fr

### Citation:

Dupré, S., Loubrieu, B., Pierre, C., Scalabrin, C., Guérin, C., Ehrhold, A., et al. (2020). The Aquitaine Shelf edge (Bay of Biscay): A primary outlet for microbial methane release. *Geophysical Research Letters*, 46, e2019GL084561  
<https://doi.org/10.1029/2019GL084561>

Received 26 JUL 2019

Accepted 15 MAR 2020

Accepted article online 28 March 2020

## The Aquitaine Shelf Edge (Bay of Biscay): A Primary Outlet for Microbial Methane Release

S. Dupré<sup>1</sup>, B. Loubrieu<sup>1</sup>, C. Pierre<sup>2</sup>, C. Scalabrin<sup>1</sup>, C. Guérin<sup>1</sup>, A. Ehrhold<sup>1</sup>, A. Ogor<sup>1</sup>, E. Gautier<sup>1</sup>, L. Ruffine<sup>1</sup>, R. Biville<sup>1</sup>, J. Saout<sup>1</sup>, C. Breton<sup>3</sup>, J. Floodpage<sup>4</sup>, and M. Lescanne<sup>4</sup>

<sup>1</sup>IFREMER, Unité Géosciences Marines, Plouzané, France, <sup>2</sup>LOCEAN/IPSL, CNRS-IRD-MNHN-Sorbonne Université, 4 place Jussieu, Paris, France, <sup>3</sup>ECCO, 1 rue de Grenoble, Maisons Alfort, France, <sup>4</sup>TOTAL SA, Centre scientifique et technique Jean-Féger, avenue Larribau, Pau, France

**Abstract** A few thousand (2,612) seeps are releasing microbial methane bubbles from the seafloor at the Aquitaine Shelf edge (Bay of Biscay) at shallow water depths (140–220 m). This methane contributes to the formation of meter-scale subcircular carbonate structures, which are (sub)outcropping over 375 km<sup>2</sup>. Based on in situ flow rate measurements and acoustic data, and assuming steady and continuous fluxes over time, the methane entering the water column is estimated at 144 Mg/yr. Microbial methane circulation has been ongoing for at least a few thousand years. This discovery highlights the importance of microbial methane generation, disconnected from deep thermogenic sources and gas hydrates, at continental shelves. The shelf edge may be viewed as a focus area for methane circulation and release and related diagenesis, all having an impact on the shaping of continental shelves and potentially on the oceanic and atmospheric carbon budget.

**Plain Language Summary** At the Aquitaine Shelf of the Bay of Biscay (Northeast Atlantic Ocean), the recent acoustic, chemical, and visual investigations of microbial methane release at the seafloor have led to the discovery of a vast fluid system. This methane escapes as bubbles from the seafloor into the seawater at 2,612 sites, all located at shallow water depths (140–220 m) along the edge of the continental shelf. Methane-derived authigenic carbonates that are by-products of gas seepage cover the (sub) seafloor over a large area of 375 km<sup>2</sup>. These carbonates form subcircular meter-scale pavements and mounds, less than 2 m in height above the surrounding seafloor. Based on the growth rate of authigenic carbonates, it can be inferred that methane circulation has occurred for at least a few thousand years. The amount of methane released from the Aquitaine Shelf seafloor into the water column, estimated at 144 t/yr, questions the fate of the methane in the ocean and its possible passage to the atmosphere with therefore consequent potential contribution to the oceanic and atmospheric carbon budget over time.

## 1. Introduction

Methane releases at continental margins are occurring worldwide, from ultrashallow to deepwater areas (Judd & Hovland, 2007). Continental shelves are important areas for organic carbon accumulation and formation of microbial methane in organic-rich sediments. Emissions of gas bubbles and dissolved methane into the water column contribute to modifying the oceanic and potentially the atmospheric carbon budget if part of this methane is released into the atmosphere (Borges et al., 2016; Hovland et al., 1993).

To map the seafloor and the water column, multibeam echosounder surveys are not generally extensively made in shallow waters as they are time-consuming. This is all the more true for wide continental shelves, such as the Aquitaine Shelf (Bellec & Cirac, 2010; Cirac et al., 1997), which extends  $60 \pm 5$  km from the coastline toward the shelf break (~220 m water depth) (Figure 1). Moreover, detecting meter-scale seafloor morphologies requires high-resolution seafloor mapping. The lack of seafloor seep-related morphologies on bathymetric maps of many shelves (Römer et al., 2017; Yun et al., 1999) may therefore simply be an apparent absence due to data resolution. Surveys conducted along the continental margins of the U.S. Atlantic (Brothers et al., 2014; Skarke et al., 2014), Cascadia (Johnson et al., 2019; Riedel et al., 2018) and Black Sea (Naudts et al., 2006) have revealed numerous seeps and seep-related structures at the shelf and upper slope domains.

Methane bubbles escaping from the seafloor at continental margins originate most of the time from a mixture of gases from deep thermogenic and shallower microbial sources, often in connection with gas hydrate

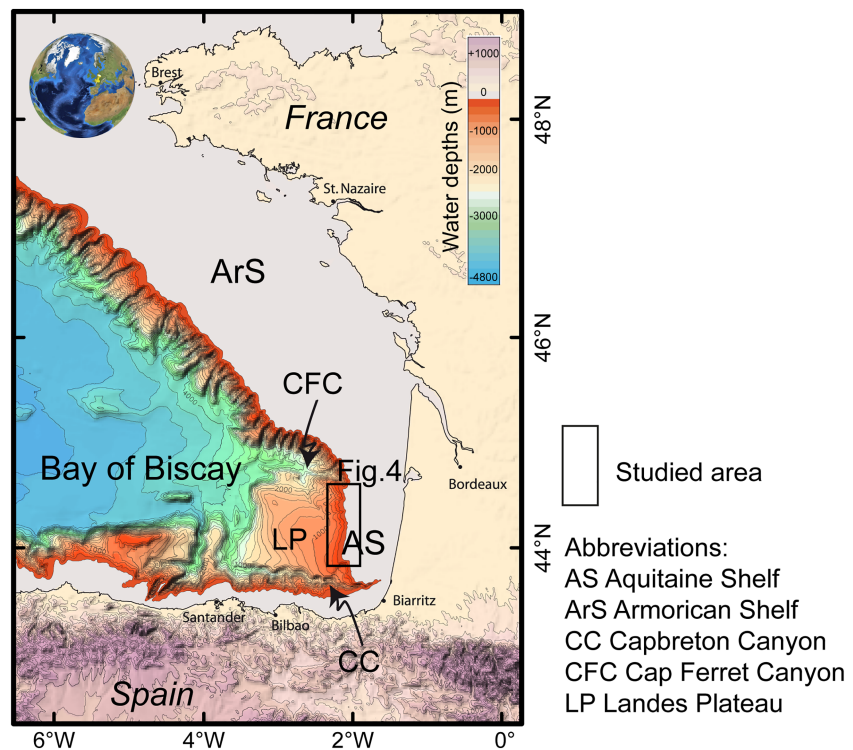


**Figure 1.** Bathymetric map of the Bay of Biscay (Northeast Atlantic Ocean) (Sibuet et al., 2004) indicating the surveyed Aquitaine Margin area.

reservoirs (Brothers et al., 2014; Johnson et al., 2015; Skarke et al., 2014). This is not the case for Aquitaine Shelf gas seeps as evidenced by molecular and isotopic ( $\delta D$  and  $\delta^{13}C$ ) analyses of gases (Ruffine et al., 2017). Gas bubbles are composed of pure microbial methane (>99.948% mol of the gases) originated from  $CO_2$  reduction, one of the main formation processes of microbial methane (Whiticar et al., 1986), and have no genetic link with thermogenic sources from the underlying Parentis Basin. This microbial methane contributes to the precipitation of Methane-Derived Authigenic Carbonates (MDACs) (Pierre et al., 2017).

The Mesozoic Aquitaine Basin located in the Bay of Biscay (Northeast Atlantic Ocean) is composed of several subbasins, including the offshore Parentis Basin (Biteau et al., 2006; Bois & Gariel, 1994) (Figure 1). The Aquitaine Shelf located partly above the Parentis Basin and Landes High is situated between two major canyons, the Cap Ferret Canyon in the north and the Capbreton Canyon in the south. The Aquitaine Shelf was mainly built by successive westward sedimentary progradations during the Oligocene, Miocene, and Pliocene (Bellec & Cirac, 2010; Cirac et al., 1997; Winnock, 1973). The uppermost sedimentary cover (1 to 2 m thick) of the Aquitaine Shelf was deposited during the Late Holocene and lies on top of soft Pleistocene sediments (Cirac et al., 2000).

For the first time, we present here the spatial distribution and geophysical signatures of the microbial methane seeps and seep-related structures of the Aquitaine Shelf, previously suspected but only in a few places (Dupré et al., 2014). The sedimentary control, the organic matter sources, and the volumes of methane emitted into the water are discussed.

## 2. Data and Methods

### 2.1. Geophysical, Sedimentological, and In Situ Data

The marine exploration expedition GAZCOGNE1 was conducted in July–August 2013 to investigate 2,100 km<sup>2</sup> of the Aquitaine Margin covering the external shelf and slope (Figure 1). The geophysical data set was acquired with ship-borne echosounders simultaneously providing acoustic images of the water column, seafloor (Figure 2), and subbottom sediments (Figure 3). Subseafloor material was collected with a

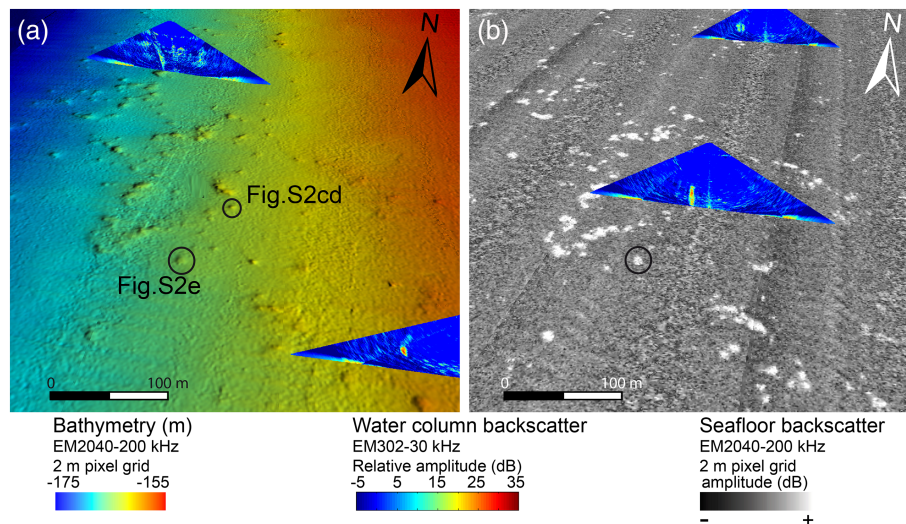


**Figure 2.** The 3-D views of a seeping area at the Aquitaine Shelf edge (Figure 4). Processed polar echograms of the water column are superimposed on high-resolution (a) shaded bathymetry and (b) seafloor backscatter. The seafloor is densely populated with carbonate mounds characterized by high-amplitude seafloor backscatter. Among the 161 seeps evidenced by water column acoustics in this area, a few tens of them were investigated during the GZ2-ROV535 dive (Figure S2).

grab sampler and a box corer (20 to 50 cm long core) to characterize the nature of outcropping rocks previously interpreted to be MDACs (Dupré et al., 2014). Thus, 27 locations distributed between 134 and 1,100 m water depths from the shelf to the slope were sampled (Figure S1a in the supporting information). During the second marine expedition GAZCOGNE2 in September 2013, the ROV (remotely operated vehicle) Victor (IFREMER) was deployed to provide ground-truth data, including in situ observations (Figure S2), samplings (gas, sediment, and carbonates), and methane flow rate measurements with the use of the Pegaz system (Lanteri & Bignon, 2007).

## 2.2. Data Processing and Interpretation

Bathymetry and seafloor backscatter data acquired with the Kongsberg EM302 (30 kHz) and EM2040 (200 kHz) multibeam echosounders were processed using Caraibes and Sonarscope software (©IFREMER). These data were combined to produce maps of morphostructures and seep-related features along the continental slope and shelf edge of the Aquitaine Margin (Figure 4). Bathymetry and backscatter resolutions of the echosounders are crucial in seafloor morphology detection. Thus, on the shelf, although the vertical resolution of the EM2040 is twice better than that of the EM302, slight depressions and reliefs (<30–40 cm) cannot be detected. Best along track bathymetric resolution on the shelf edge ranges from 1.2 to 3 m for incidence angles <50°, while across-track resolution decreases from 2.4 m vertically below the ship to 10 m at a 50° incidence angle. Seafloor backscatter maps, with a better across track resolution (increasing with the incidence angle) than that of bathymetry maps, are very well suited to complete the bathymetric mapping. They are particularly efficient in identifying carbonates outcropping at the seafloor and those slightly buried (<1 m below the seafloor) within the sediment (Dupré et al., 2010). The carbonates are characterized by high-amplitude seafloor backscatter providing a strong amplitude contrast with surrounding sediment (Figure 2b), facilitating their identification (Text S1). MDACs were reliably mapped using acoustic signatures of ground-truth features (Figure S2). Indeed, near-bottom observations and sampling with the ROV have confirmed their authigenic origin and their relation with the microbial methane seeps, inferred from their mineralogical and isotopic compositions (Pierre, Demange, et al., 2017).

Processing and interpretation of the multibeam water column data were performed with Sonarscope and Globe/3DViewer software (Augustin, 2011; Dupré et al., 2015; Poncelet et al., 2015) and have led to provide the first accurate spatial distribution of the gas-bubbling sites over the Aquitaine Shelf and slope (Figure 4a). In echograms, gas bubbles form so-called acoustic gas “plumes” (Merewether et al., 1985) or gas “flares” (Obzhirov et al., 2004), resulting from the impedance contrast between gas and seawater. Gas bubble echoes have very high amplitudes, a few tens of dB higher than the background seawater (Figure 2). Near-bottom

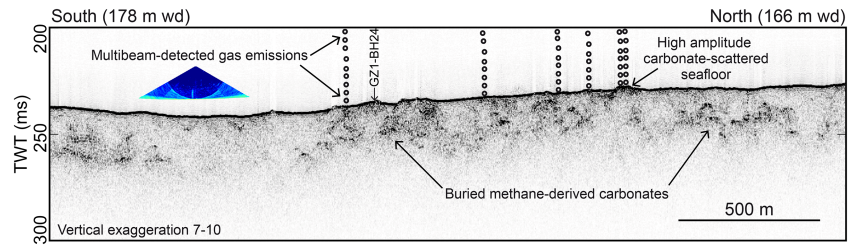


**Figure 3.** Subbottom profile across seeping sites at the Aquitaine Shelf edge (Figure 4a). Grab sampling along this profile (GZ1-BH24) recovered authigenic carbonates (Pierre, Demange, et al., 2017). Gas emissions, along the profile and within its close vicinity (less than 20 m), are reported.

visual surveys with the ROV confirmed gas bubbles escaping from the seabed at these locations (Figure S2). Gas emission mapping is based on the complete EM302 water column data set with the exclusion of acoustic signatures of biomass (shoals of fish, plankton) (Dupré et al., 2014).

The sedimentary facies map of the Aquitaine Shelf edge and slope (Figure 4b) was based on EM302 seafloor backscatter classification (Figure S1b) calibrated with sediment samples. The sediments were analyzed and classified based on nomenclatures from Folk (1984) and Lesueur and Klingébiel (1986).

Subbottom profiler data recorded along 2,771 km with a hull-mounted Echoes 3500 (1.8–5.3 kHz) were validated, processed, and replayed with Subop-Acquisition and QC-Subop software (©IFREMER) (Figure 3). The vertical resolution of these seismic data approximates 30 cm with a horizontal resolution of 15 m in the shelf area.

### 3. Fluid Systems Offshore the Aquitaine Margin

The Aquitaine continental slope ( $3^\circ$ ) is cut off north of latitude  $44^\circ 10' N$  by several canyons clearly exposed in the bathymetry by major incisions (e.g., Arcachon Canyon). The southern part is characterized by sediment waves (Faugères et al., 2002) and the Capbreton slide (Figure 4).

#### 3.1. MDACs (Sub)outcropping Over 375 km<sup>2</sup> of the Shelf Edge

The seafloor backscatter signature of carbonates corresponds almost exclusively to meter-scale subcircular patches primarily arranged in clusters (Figure 2). They consequently form (sub)outcropping structures from a few tens to 120 m long. The carbonates are exclusively located along the shelf edge with the majority (98%) between 140 and 220 m water depths (Figure 4a). The (sub)outcropping carbonates, accounting for 30 km<sup>2</sup>, are spread over a 375 km<sup>2</sup> area that extends over a distance of 80 km between the Cap Ferret and Capbreton canyons. The western spatial limit of the MDACs coincides with the shelf break. Where the shelf edge is indented by canyons (north of latitude  $44^\circ 10' N$ ), their eastern limit varies significantly. Thus, in the inter-canyon domain, the carbonates extend further east (up to ~8 km) than in front of the canyon heads where only a small number of carbonate structures is present (a few hundreds of meters eastward). In contrast, where the shelf edge is not disturbed by canyons (south of latitude  $44^\circ 10' N$ ), the MDAC distribution is much more extensive, with a carbonate area 3 times larger than in the north and gathering more than 80% of total identified carbonates.

Four distinct seafloor backscatter facies associated with specific seafloor morphologies characterize these carbonates. The dominant facies corresponds to meter-scale patches of high-amplitude backscatter that are outcropping from the surrounding sediments by only a few tens of decimeters, just below the threshold detection of the echosounders. Nevertheless, some meter-scale carbonates sufficiently outcrop from the sediments to be detected in EM2040 bathymetry (second facies). These morphological structures are described hereafter as carbonate mounds, and there are 2,724 of them in total. The majority (90%) are 0.5 to 1.5 m high and do not exceed 2 m above the seafloor. The carbonate mounds have the highest seafloor backscatter amplitude of all the carbonates, with a mean relative value of  $-16$  and  $-14$  dB in EM302 and EM2040 data, respectively. These mounds, located between 141 and 223 m water depths, cover only 15% of the total carbonate area. Most of the carbonate mounds are located in the southern Aquitaine Shelf (south of latitude  $44^\circ 10' N$ ) and are mainly distributed in the northern half along a 22 km long NS oriented band within which

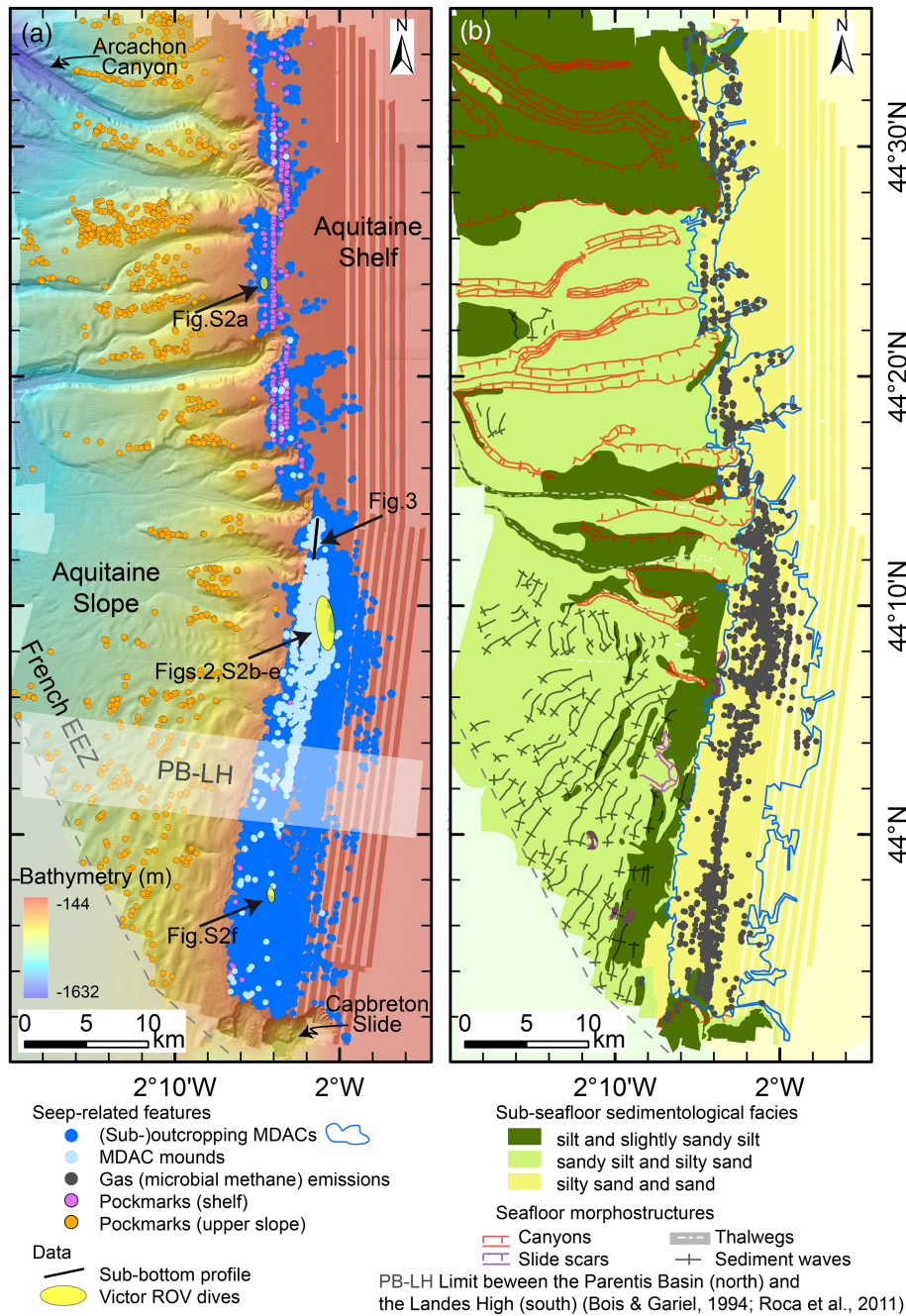


**Figure 4.** Detailed (a) shaded bathymetric and (b) subseafloor sedimentological maps of the Aquitaine Shelf edge area with indication of methane emissions, seep-related features, and seafloor morphological structures.

mound density reaches  $180/\text{km}^2$ . The third acoustic facies corresponds to smaller subcircular backscatter patches, mainly isolated from each other, and ranging from a few to 10 m in diameter. They are not associated with detectable morphology and are mainly observed north of latitude  $44^\circ 10' \text{N}$ . The fourth acoustic facies characterizes the carbonates with meter-scale patches of irregular contours and medium-amplitude backscatter. This facies most likely corresponds to carbonates that are either partially covered by sediments or slightly buried within the uppermost sediments. These features are present only in the southern Aquitaine Shelf and mainly in the most eastern part of the carbonate field.

Subbottom profiles exhibit strong amplitudes at the seabed and in the sedimentary strata down to 20–30 m maximum below the seafloor (Figure 3). The strong amplitudes at the seafloor are the acoustic signature of

(sub)outcropping carbonates, as was evidenced through in situ observations (Figure S2), samplings (Pierre, Demange, et al., 2017), and the inability to conduct coring due to the presence of buried carbonates. Due to the similarity in acoustic facies (amplitude and shape) between the anomalies at the seafloor and within the sedimentary strata, the high-amplitude reflections in-depth are interpreted to be caused by buried carbonates. The presence of local gas accumulations cannot however be ruled out and could contribute to the enhancement of the amplitudes. A maximum penetration of 80 m is observed in undisturbed sedimentary areas, while the penetration does not exceed 40 m in the fluid-disturbed area.

### 3.2. Two Distinct Families of Pockmarks in the Slope and Shelf Domains

Two distinct families of depressions are present in the Aquitaine Shelf and slope differing in location and size (Figure 4a). The first group comprises 826 depressions of 100 to 200 m in diameter and 15 m in depth on average. These large pockmarks are exclusively located along the continental slope mainly below 350 m water depth (Michel et al., 2017). A second group of 696 depressions, mapped by means of high-resolution bathymetry, is present on the shelf, with small dimensions of less than 5 m in diameter on average with a depth of less than 30–40 cm. However, it cannot be excluded that small-scale pockmarks are present in the slope domain. Only a few meter-scale pockmarks were detected in the upper slope where the data resolution permits. The small-scale pockmarks on the shelf are almost exclusively (99.4%) located north of latitude 44°10'N at water depths ranging between 151 and 224 m. The majority of these pockmarks are not detectable in seafloor backscatter data because of amplitudes similar to those of surrounding sediment. Although a few of these depressions are located at the edge of carbonate structures, most of them are isolated features.

### 3.3. A Few Thousand Microbial Methane Emissions at the Shelf Edge

Up to 2612 gas emission sites were acoustically identified (Figure 4b). Acoustic “flares” formed by escaping gas bubbles are mostly subvertical, sometimes deviated by currents (Figure 2). Clearly originating from the seafloor, these acoustic “flares” rise from a few tens of meters above the seafloor up to the seawater-atmosphere interface. The methane flow rate, measured at the seafloor with the inverted funnel of the Pegaz sampler at nine locations, varies from 35 to 368 ml/min (Ruffine et al., 2017). These volumes are normalized to standard atmospheric conditions for comparison purpose of gas discharge at different water depths. These measured methane flow rates are positively correlated with the intensity (amplitude) and height of the acoustic water column anomalies, allowing to estimate the total volume of methane emitted into the water at  $212 \times 10^6$  L/yr (normalized to standard atmospheric conditions) assuming steady and continuous fluxes over time (corroborated by acoustic water column records back to 1998, Dupré et al., 2014). This estimation takes into account the flux variability and corresponds to an annual methane flow rate of 144 Mg/yr. The majority of seeping sites coincide with areas of strong seafloor backscatter. Emission sites are located either within these high-amplitude patches (24%) or in their close periphery, 10 to 150 m distance from them (54%). Slightly more than one third of the carbonate mounds are active sites (980 structures). One third of gas emissions occur through carbonate crusts, while the other two thirds are located in the very close periphery of the carbonate mounds, within a 20 m distance from their borders. In contrast, only 12% (48 depressions) of the pockmarks are active. With no indication of the presence of MDACs, inactive and active pockmarks on the shelf could be recent and nascent, respectively. Almost all (99.5%) gas emissions are located along the edge of the continental Aquitaine Shelf between 139 and 220 m water depths. The seepage area is quasi-exclusively comprised within the MDAC-scattered (sub)seafloor. Both areas roughly coincide in the north where the shelf edge is indented by canyons, whereas the carbonate area is larger than the seeping area in the south where present-day inactive carbonate structures are present a few kilometers west and east from the seeps. Seep density is higher south of latitude 44°13.96'N with up to 88 seeping sites per square kilometer. Canyons indenting the shelf edge and the Capbreton slide are both free of seeps with only a few exceptions in one of the canyon heads (latitude 44°14.9'N) and along the northern border of the Capbreton slide.

## 4. Discussion and Conclusion

Unprecedented high-resolution acoustic data have confirmed the existence of persistent gas releases and MDACs only at the Aquitaine Shelf edge (Dupré et al., 2014). This has made way to the discovery of an unknown widespread active and fossil fluid system exclusively associated with microbial methane (Pierre,

Demange, et al., 2017; Ruffine et al., 2017). MDACs are present over an area of 375 km<sup>2</sup> extending from the Cap Ferret to the Capbreton canyons and are associated with more than 2,600 gas bubble streams.

The spatial distribution of seeps and seep-related features does not evidence any tectonic control and no preferential localization along preexisting regional faults (e.g., W-E oriented normal faults, Ferrer et al., 2008; Roca et al., 2011). The microbial methane system is not delineated by specific structural features but overlays both the Parentis Basin and the Landes High (Dupré et al., 2014). The microbial methane has neither a genetic link with thermogenic hydrocarbons from the Parentis Basin beneath nor is it linked to gas hydrate dissociation (Ruffine et al., 2017). With the chemical composition of this gas, the temperature, pressure, and salinity conditions from the shelf (12.3 °C and a salinity of 35.1 PSU at 150 m water depth), the slope (11.4 °C and a salinity of 35.4 PSU at 475 m water depth), the deeper part (8.8 °C at 1200 m water depth) (Marié et al., 2019), and a geothermal gradient of 24 °C/km, calculation using a well-proven model (Sun & Duan, 2007) shows that the shelf and upper slope along the Aquitaine Margin is clearly outside the gas hydrate stability zone.

Seeps and MDACs are absent from the slope, the shelf-indenting canyons, and the Capbreton slide and are restricted to the Aquitaine Shelf edge with no other evidence detected or reported so far, for example, along the Armorican Shelf. The sedimentary levels containing the organic matter from which microbial methane is generated could be located beyond the shelf break with methane possibly rising along the slope or at the shelf level below the seepage and carbonate area. The microbial methane could originate from the Plio-Pleistocene and Holocene deposits in relation to the high sedimentary and organic supplies recorded during these periods (Cremer, 1983) that would have favored microbial methanogenesis. These deposits are well preserved at the shelf. However, based on the temperature range for microbial methane genesis (Katz, 2011) and the regional geothermal gradient (Biteau et al., 2006), it cannot be excluded that the emitted microbial methane originates from deeper sedimentary levels. Offshore Japan, microbial methane genesis by CO<sub>2</sub> reduction has been identified in lignite coal beds between 1.5 and 2.5 km below the seafloor (Inagaki et al., 2015). Seepage activity is more intense south of latitude 44°10'N where seeps and suboutcropping carbonates are much more numerous and widespread. These differences could reflect the presence of sedimentary source levels that may be thicker and/or richer in organic matter in the south than in the north. Investigations in seismics, coring, and drilling are required to precisely characterize the source levels of the emitted microbial methane.

The seafloor morphology of the Aquitaine Shelf edge is strongly dominated by thick suboutcropping MDACs, whose formation is driven by moderate and long-term continuous methane fluxes. Far less abundant and of much smaller size, the pockmarks highlight locally focused fluid outlets. Considering the maximum carbonate thickness (from 2 to 8 m inferred from in situ observations and seismic data, respectively) and the possible range for carbonate growth rate (from 4 to 1,200 mm/ky, Bayon et al., 2009; Liebetau et al., 2014) and assuming continuous fluxes over time, they may have formed at least a few thousand years ago.

On the Aquitaine Shelf, despite numerous MDACs, microbial methane is not totally consumed by anaerobic oxidation of methane as evidenced by gas emissions in the water column. The methane concentrations are high enough to form gas bubbles which are emitted into the water column at an annual methane flow rate estimated at 144 Mg/yr. This methane flow rate is within the range (~4 to 500 Mg/yr) of other estimates at shallow water seeping sites of similar tectonic setting (Table S1) (Greinert et al., 2010; Riedel et al., 2018; Römer et al., 2017; Schneider von Deimling et al., 2011; Skarke et al., 2014; Veloso-Alarcón et al., 2019). The seep distribution over 375 km<sup>2</sup> gives an advective flux of 0.38 CH<sub>4</sub> g/m<sup>2</sup>/yr. To estimate the total volume of microbial methane generated, the volume of methane entering the water column by advection and diffusion, the volume of methane required for carbonate precipitation via anaerobic oxidation of methane, and the volume of methane potentially trapped in depth in the sedimentary strata have all to be considered. Further investigation involving new acquisitions (samples and seismics) would be required to reasonably assess these volumes.

The discovery of widespread and persistent methane emissions at shallow water depths along the edge of the Aquitaine Shelf (140–220 m water depth) also questions the fate of methane in the water through dissolution (Olsen et al., 2019), aerobic oxidation via microbial processes (Kelley, 2003), and transfer to the atmosphere (Römer et al., 2017) with potential contribution to the global atmospheric methane budget.



Although the Aquitaine Shelf microbial methane system presents some similarities with other shallow water sites (Baraza & Ercilla, 1996; García-García et al., 2007; Johnson et al., 2019; Jones et al., 2012; Naudts et al., 2006; Prouty et al., 2016; Schattner et al., 2012; Yun et al., 1999), it represents a unique case at continental shelves with regard to (1) the nature and origin of the fluids (pure microbial methane not related to gas hydrates); (2) the presence of seeps and related MDACs over a large area (375 km<sup>2</sup>) with a good state of preservation over time, attesting to the persistence of methane circulation through time; (3) and the amount of released methane at the seafloor (144 Mg/yr). The discovery of the Aquitaine Shelf microbial methane system identifies and highlights the edge of the shelf as a privileged area for microbiogeological processes.

In light of our study and recent discoveries in particular along the U.S. Atlantic and Cascadia margins, continental shelf edges around the world may be seen as primary outlets for microbial methane releases, independently of the prevalent tectonic regime and the presence of gas hydrates (Johnson et al., 2015; Prouty et al., 2016). Microbial methane circulation might play a predominant role in the shaping and evolution of the shelf edge in interactions with offshore groundwater discharge (Hong et al., 2019; Pierre et al., 2017; Pierre, Demange, et al., 2017) and possibly but not necessary with gas hydrate dissociation (Johnson et al., 2019; Skarke et al., 2014).

#### Acknowledgments

We are grateful to the officers and crews of the research vessels Le Suroit and Pourquoi pas ? and the Victor ROV team. We would like to thank Mathilde Pitel, Arnaud Gaillot, and Elodie Petit for their assistance in data processing and Jean-François Bourillet, Philippe Bourges, and Jean-Noël Ferry for conducting the PAMELA (PAssive Margin Exploration Laboratories) project. This study and the marine expeditions GAZCOGNE1 (<https://doi.org/10.17600/13020070>) and GAZCOGNE2 (<https://doi.org/10.17600/13030090>) were cofunded by TOTAL and IFREMER. We thank Alison Chalm for language corrections and Wei-Li Hong and Marc De Batist for their constructive reviews.

#### References

- Augustin, J.-M. (2011). Developing and deploying sonar and echosounder data analysis software. *Matlab Newsletters*. Retrieved from Matlab website: <http://www.mathworks.fr/company/newsletters/articles/developing-and-deploying-sonar-and-echosounder-data-analysis-software.html>
- Baraza, J., & Ercilla, G. (1996). Gas-charged sediments and large pockmark-like features on the Gulf of Cadiz slope (SW Spain). *Marine and Petroleum Geology*, 13(2), 253–261. [https://doi.org/10.1016/0264-8172\(95\)00058-5](https://doi.org/10.1016/0264-8172(95)00058-5)
- Bayon, G., Henderson, G. M., & Bohn, M. (2009). U-Th stratigraphy of a cold seep carbonate crust. *Chemical Geology*, 260(1–2), 47–56. <https://doi.org/10.1016/j.chemgeo.2008.11.020>
- Bellec, V. K., & Cirac, P. (2010). Internal architecture of the soft sediment cover of the South-Aquitaine shelf (Bay of Biscay): A record of high frequency sea level variations? *Comptes Rendus Geoscience*, 342(1), 79–86. <https://doi.org/10.1016/j.crte.2009.09.007>
- Biteau, J.-J., Le Marrec, A., Le Vot, M., & Masset, J.-M. (2006). The Aquitaine Basin. *Petroleum Geoscience*, 12(3), 247–273. <https://doi.org/10.1144/1354-079305-674>
- Bois, C., & Gariel, O. (1994). Deep seismic investigation on the Parentis basin (Southwestern France). In A. Mascle (Ed.), *Hydrocarbon and petroleum geology of France, Special publication of the European Association of Petroleum Geologists* (Vol. 4, pp. 173–186). Berlin: Springer, Berlin, Heidelberg.
- Borges, A. V., Champenois, W., Gypens, N., Delille, B., & Harlay, J. (2016). Massive marine methane emissions from near-shore shallow coastal areas. *Scientific Reports*, 6(1), 1–8. <https://doi.org/10.1038/srep27908>
- Brothers, D. S., Ruppel, C., Kluesner, J. W., ten Brink, U. S., Chaytor, J. D., Hill, J. C., et al. (2014). Seabed fluid expulsion along the upper slope and outer shelf of the U.S. Atlantic continental margin. *Geophysical Research Letters*, 41, 96–101. <https://doi.org/10.1002/2013gl058048>
- Cirac, P., Berné, S., Castaing, P., & Weber, O. (2000). Sedimentary processes and facies on the northern Aquitaine shelf, France. *Processus de mise en place et d'évolution de la couverture sédimentaire superficielle de la plate-forme nord-aquitaine. Oceanologica Acta*, 23(6), 663–686. [https://doi.org/10.1016/s0399-1784\(00\)00110-9](https://doi.org/10.1016/s0399-1784(00)00110-9)
- Cirac, P., Berné, S., Lericolais, G., & Weber, O. (1997). Late Quaternary depositional sequence on the north Aquitaine continental shelf (Atlantic ocean, France). *Bulletin de la Société Géologique de France*, 168(6), 717–725.
- Cremer, M. (1983). Approches sédimentologique et géophysique des accumulations turbiditiques: l'éventail profond du Cap-Ferret (Golfe de Gascogne), la série des grès d'Annot (Alpes-de-Haute-Provence). Thèse de doctorat de l'Université Bordeaux 1, Retrieved from <https://tel.archives-ouvertes.fr/tel-00694901>, 419 pp.
- Dupré, S., Berger, L., Le Bouffant, N., Scalabrin, C., & Bourillet, J.-F. (2014). Fluid emissions at the Aquitaine Shelf (Bay of Biscay, France): A biogenic origin or the expression of hydrocarbon leakage? *Continental Shelf Research*, 88, 24–33. <https://doi.org/10.1016/j.csr.2014.07.004>
- Dupré, S., Scalabrin, C., Grall, C., Augustin, J. M., Henry, P., Şengör, A. M. C., et al. (2015). Tectonic and sedimentary controls for wide-spread gas emissions in the Sea of Marmara. Results from systematic, shipborne multibeam echosounder water column imageries. *Journal of Geophysical Research: Solid Earth*, 120, 2891–2912. <https://doi.org/10.1002/2014JB011617>
- Dupré, S., Woodside, J., Klauke, I., Mascle, J., & Foucher, J.-P. (2010). Widespread active seepage activity on the Nile Deep Sea Fan (offshore Egypt) revealed by high-definition geophysical imagery. *Marine Geology*, 275(1–4), 1–19. <https://doi.org/10.1016/j.margeo.2010.04.003>
- Faugères, J. C., Gonthier, E., Mulder, T., Kenyon, N., Cirac, P., Gribouard, R., et al. (2002). Multi-process generated sediment waves on the Landes Plateau (Bay of Biscay, North Atlantic). *Marine Geology*, 182(3–4), 279–302. [https://doi.org/10.1016/S0025-3227\(01\)00242-0](https://doi.org/10.1016/S0025-3227(01)00242-0)
- Ferrer, O., Roca, E., Benjumea, B., Munoz, J. A., Ellouz, N., & the Marconi Team (2008). The deep seismic reflection MARCONI-3 profile: Role of extensional Mesozoic structure during the Pyrenean contractional deformation at the eastern part of the Bay of Biscay. *Marine and Petroleum Geology*, 25(8), 714–730. <https://doi.org/10.1016/j.marpetgeo.2008.06.002>
- Folk, R. (1984). The distinction between grain size and mineral composition in sedimentary-rock nomenclature. *The Journal of Geology*, 62(4), 344–359.
- García-García, A., Orange, D. L., Miserocchi, S., Correggiari, A., Langone, L., Lorenson, T. D., et al. (2007). What controls the distribution of shallow gas in the Western Adriatic Sea? *Continental Shelf Research*, 27(3–4), 359–374. <https://doi.org/10.1016/j.csr.2006.11.003>
- Greiner, J., McGinnis, D. F., Naudts, L., Linke, P., & De Batist, M. (2010). Atmospheric methane flux from bubbling seeps: Spatially extrapolated quantification from a Black Sea shelf area. *Journal of Geophysical Research*, 115, C01002. <https://doi.org/10.1029/2009jc005381>

- Hong, W. L., Lepland, A., Himmler, T., Kim, J. H., Chand, S., Sahy, D., et al. (2019). Discharge of meteoric water in the eastern Norwegian Sea since the last glacial period. *Geophysical Research Letters*, *46*, 8194–8204. <https://doi.org/10.1029/2019gl084237>
- Hovland, M., Judd, A. G., & Burke, R. A. (1993). The global flux of methane from shallow submarine sediments. *Chemosphere*, *26*(1–4), 559–578. [https://doi.org/10.1016/0045-6535\(93\)90442-8](https://doi.org/10.1016/0045-6535(93)90442-8)
- Inagaki, F., Hinrichs, K.-U., Kubo, Y., Bowles, M. W., Heuer, V. B., Hong, W.-L., et al. (2015). Exploring deep microbial life in coal-bearing sediment down to ~2.5 km below the ocean floor. *Science*, *349*(6246), 420–424. <https://doi.org/10.1126/science.aaa6882>
- Johnson, H. P., Merle, S., Salmi, M., Embley, R., Sampaga, E., & Lee, M. (2019). Anomalous concentration of methane emissions at the continental shelf edge of the northern Cascadia Margin. *Journal of Geophysical Research: Solid Earth*, *124*, 2829–2843. <https://doi.org/10.1029/2018jb016453>
- Johnson, H. P., Miller, U. K., Salmi, M. S., & Solomon, E. A. (2015). Analysis of bubble plume distributions to evaluate methane hydrate decomposition on the continental slope. *Geochemistry, Geophysics, Geosystems*, *16*, 3825–3839. <https://doi.org/10.1002/2015gc005955>
- Jones, D. T., Wilson, C. D., De Robertis, A., Rooper, C. N., Weber, T. C., & Butler, J. L. (2012). Evaluation of rockfish abundance in untrawlable habitat: Combining acoustic and complementary sampling tools. *Fishery Bulletin*, *110*(3), 332–343.
- Judd, A. G., & Hovland, M. (2007). *Seabed fluid flow. The impact on geology, biology and the marine environment* (p. 293). Cambridge: Cambridge University Press.
- Katz, B. J. (2011). Microbial processes and natural gas accumulations. *The Open Geology Journal*, *5*, 75–83. <https://doi.org/10.2174/1874262901105010075>
- Kelley, C. (2003). Methane oxidation potential in the water column of two diverse coastal marine sites. *Biogeochemistry*, *65*(1), 105–120. <https://doi.org/10.1023/a:1026014008478>
- Lanteri, N., & Bignon, L. (2007). Device for taking pressurized samples, European Patent WO/2007/128891.
- Lesueur, P., & Klingébiel, A. (1986). Carte et notice de répartition des sédiments superficiels du plateau continental du Golfe de Gascogne, partie septentrionale (éch.: 1/500 000). Coédition BRGM/IFREMER Carte géologique de la marge continentale française 1. CIESM Editions.
- Liebetrau, V., Augustin, N., Kutterolf, S., Schmidt, M., Eisenhauer, A., Garbe-Schönberg, D., & Weinrebe, W. (2014). Cold-seep-driven carbonate deposits at the Central American forearc: Contrasting evolution and timing in escarpment and mound settings. *International Journal of Earth Sciences*, *103*(7), 1845–1872. <https://doi.org/10.1007/s00531-014-1045-2>
- Marié, L., Loubrieu, B., & Dupré, S. (2019). Seawater temperature, conductivity, pressure and salinity data offshore the Aquitaine Basin (XBT profiles and near-bottom moorings). SEANO database. <https://doi.org/10.17882/61855>
- Merewether, R., Olsson, M. S., & Lonsdale, P. (1985). Acoustically detected hydrocarbon plumes rising from 2-km depths in Guaymas Basin, Gulf of California. *Journal of Geophysical Research*, *90*(B4), 3075–3085. <https://doi.org/10.1029/JB090iB04p03075>
- Michel, G., Dupré, S., Baltzer, A., Ehrhold, A., Imbert, P., Pitel, M., et al. (2017). Pockmarks on the South Aquitaine Margin continental slope: The seabed expression of past fluid circulation and former bottom currents. *Comptes Rendus Geoscience*, *349*(8), 391–401. <https://doi.org/10.1016/j.crte.2017.10.003>
- Naudts, L., Greinert, J., Artemov, Y., Staelens, P., Poort, J., Van Rensbergen, P., & De Batist, M. (2006). Geological and morphological setting of 2778 methane seeps in the Dnepr paleo-delta, northwestern Black Sea. *Marine Geology*, *227*(3–4), 177–199. <https://doi.org/10.1016/j.margeo.2005.10.005>
- Obzhairov, A., Shakirov, R., Salyuk, A., Suess, E., Biebow, N., & Salomatin, A. (2004). Relations between methane venting, geological structure and seismo-tectonics in the Okhotsk Sea. *Geo-Marine Letters*, *24*, 135–139. <https://doi.org/10.1007/s00367-004-0175-0>
- Olsen, J. E., Krause, D. F., Davies, E. J., & Skjetne, P. (2019). Observations of rising methane bubbles in Trondheimsfjord and its implications to gas dissolution. *Journal of Geophysical Research: Oceans*, *124*, 1399–1409. <https://doi.org/10.1029/2018jc013978>
- Pierre, C., Blanc-Valleron, M.-M., Boudouma, O., & Lofi, J. (2017). Carbonate and silicate cementation of siliciclastic sediments of the New Jersey shelf (IODP Expedition 313): Relation with organic matter diagenesis and submarine groundwater discharge. *Geo-Marine Letters*, *37*(6), 537–547. <https://doi.org/10.1007/s00367-017-0506-6>
- Pierre, C., Demange, J., Blanc-Valleron, M.-M., & Dupré, S. (2017). Authigenic carbonate mounds from active methane seeps on the southern Aquitaine Shelf (Bay of Biscay, France): Evidence for anaerobic oxidation of biogenic methane and submarine groundwater discharge during formation. *Continental Shelf Research*, *133*, 13–25. <https://doi.org/10.1016/j.csr.2016.12.003>
- Poncelet, C., Sinquin, J.-M., Loubrieu, B., Corre, M.-P., Dupré, S., et al. (2015). GLOBE software. Paper presented at the MeriGéo, Brest, 24–26 novembre 2015. Retrieved from [https://www.merigeo.fr/content/download/93156/file/posterMeriGeo\\_Poncelet\\_al.pdf](https://www.merigeo.fr/content/download/93156/file/posterMeriGeo_Poncelet_al.pdf)
- Prouty, N. G., Sahy, D., Ruppel, C. D., Roark, E. B., Condon, D., Brooke, S., et al. (2016). Insights into methane dynamics from analysis of authigenic carbonates and chemosynthetic mussels at newly-discovered Atlantic Margin seeps. *Earth and Planetary Science Letters*, *449*, 332–344. <https://doi.org/10.1016/j.epsl.2016.05.023>
- Riedel, M., Scherwath, M., Römer, M., Veloso, M., Heesemann, M., & Spence, G. D. (2018). Distributed natural gas venting offshore along the Cascadia margin. *Nature Communications*, *9*(1), 1–14. <https://doi.org/10.1038/s41467-018-05736-x>
- Roca, E., Munoz, J. A., Ferrer, O., & Ellouz, N. (2011). The role of the Bay of Biscay Mesozoic extensional structure in the configuration of the Pyrenean orogen: Constraints from the MARCONI deep seismic reflection survey. *Tectonics*, *30*, TC2001. <https://doi.org/10.1029/2010tc002735>
- Römer, M., Wenau, S., Mau, S., Veloso, M., Greinert, J., Schlüter, M., & Bohrmann, G. (2017). Assessing marine gas emission activity and contribution to the atmospheric methane inventory: A multidisciplinary approach from the Dutch Dogger Bank seep area (North Sea). *Geochemistry, Geophysics, Geosystems*, *18*, 2617–2633. <https://doi.org/10.1002/2017GC006995>
- Ruffine, L., Donval, J.-P., Croguennec, C., Bignon, L., Birot, D., Battani, A., et al. (2017). Gas seepage along the edge of the Aquitaine shelf (France): Origin and local fluxes. *Geofluids*, *2017*, 1–13. <https://doi.org/10.1155/2017/4240818>
- Schattner, U., Lazar, M., Harari, D., & Waldmann, N. (2012). Gas migration systems offshore northern Israel, first evidence from seafloor and subsurface data. *Continental Shelf Research*, *48*, 167–172. <https://doi.org/10.1016/j.csr.2012.08.003>
- Schneider von Deimling, J., Rehder, G., Greinert, J., McGinnis, D. F., Boetius, A., & Linke, P. (2011). Quantification of seep-related methane gas emissions at Tommeliten, North Sea. *Continental Shelf Research*, *31*(7–8), 867–878. <https://doi.org/10.1016/j.csr.2011.02.012>
- Sibuet, J.-C., Monti, S., Loubrieu, B., Mazé, J.-P., & Srivastava, S. (2004). Bathymetric map of the NE Atlantic Ocean and Bay of Biscay: Kinematic implications. *Bulletin de la Société Géologique de France*, *175*(5), 429–442. <https://doi.org/10.2113/175.5.429>
- Skarke, A., Ruppel, C., Kodis, M., Brothers, D., & Lobecker, E. (2014). Widespread methane leakage from the sea floor on the northern US Atlantic margin. *Nature Geoscience*, *7*(9), 657–661. <https://doi.org/10.1038/ngeo2232>
- Sun, R., & Duan, Z. (2007). An accurate model to predict the thermodynamic stability of methane hydrate and methane solubility in marine environments. *Chemical Geology*, *244*(1), 248–262. <https://doi.org/10.1016/j.chemgeo.2007.06.021>

- Veloso-Alarcón, M. E., Jansson, P., de Batist, M., Minshull, T. A., Westbrook, G. K., Pälke, H., et al. (2019). Variability of acoustically evidenced methane bubble emissions offshore Western Svalbard. *Geophysical Research Letters*, *46*, 9072–9081. <https://doi.org/10.1029/2019gl082750>
- Whiticar, M. J., Faber, E., & Schoell, M. (1986). Biogenic methane formation in marine and freshwater environments: CO<sub>2</sub> reduction vs. acetate fermentation—Isotope evidence. *Geochimica et Cosmochimica Acta*, *50*(5), 693–709. [https://doi.org/10.1016/0016-7037\(86\)90346-7](https://doi.org/10.1016/0016-7037(86)90346-7)
- Winnock, E. (1973). Exposé succinct de l'évolution paléogéologique de l'Aquitaine. *Bulletin de la Société Géologique de France*, *S7*, 5–12.
- Yun, J. W., Orange, D. L., & Field, M. E. (1999). Subsurface gas offshore of northern California and its link to submarine geomorphology. *Marine Geology*, *154*(1), 357–368. [https://doi.org/10.1016/S0025-3227\(98\)00123-6](https://doi.org/10.1016/S0025-3227(98)00123-6)